Dynamics of Linear Systems with Semiactive Force Generators

Ross R. Allen*
University of California, Los Angeles, Calif.

A semiactive element produces control forces in a dynamic system by controlled variation of a resistive parameter. Control constraints exist making the output of a semiactive element complex and nonlinear even for linear feedback control laws. State equations are derived for a general linear system with an arbitrary number of semiactive elements. These equations are piecewise-linear and exhibit intermittent linear dependencies among elements of the state vector. Two special cases exist yielding simplified descriptions of the semiactive control and system dynamics. Semiactive vibration control is applied to a flexible vehicle on a rough guideway. Numerical results demonstrate performance superior to passive suspensions and comparable to fully-active control.

Introduction

APPLICATION of modern control theory and parameter optimization techniques to shock and vibration control permit the design of high-performance suspension systems for taxiing aircraft[1] and ground vehicles.[2-7] Due to their simplicity, low cost, and reliability, passive suspensions composed of spring and damper elements are used in all but the most critical applications. Although control using active force generators receives considerable attention in the literature, its superior performance over passive control is frequently offset in practical designs by increased cost, complexity, energy requirements, and weight. While passive devices are self-powered and self-contained, an active force generator requires a power source to generate control inputs along with measurement and signal-processing systems. At least the disadvantages of a power supply can be eliminated by parametric control in which the parameters of passive elements are varied in response to a control signal. When a resistive parameter is varied, large control forces in a dynamic system may be generated by controlled dissipation of system energy. This type of control, which has been called *semiactive*,[8] combines features of passive control with the capability of generating the sophisticated feedback controls usually reserved for active systems.

Recently, semiactive control has been studied in shock and vibration applications.[8-11] In linear and nonlinear systems with deterministic[8-10] and random inputs,[9-11] these studies have established that the performance of semiactive force generators approaches that of fully active elements. This is not too surprising because any stable vibration-control system must eventually dissipate system vibrational energy, something a resistor does quite well. Although these studies illustrate basic applications and principles of semiactive control, a general treatment of the dynamics of a system with an arbitrary number of semiactive elements is lacking. Semiactive control introduces complex, nonstationary dynamics in even simple, linear systems.[8,9] Because control forces are produced by a dissipative process, an inequality constraint on control power exists causing complex behavior of the semiactive control force. In this paper, a general theory of the dynamics of systems with semiactive elements is developed. Two special cases are found that provide simplified representations of the semiactive control and system dynamics.

Received July 6, 1976.
Index categories: Navigation, Control, and Guidance Theory; Aircraft Vibration.

*Assistant Professor, Mechanics and Structures Department.

General Theory

In Fig. 1, a control element within a dynamic system is shown schematically along with its bond graph representation as a one-port, controlled force generator (SE).[12] In response to a *control signal* $e(t)$, the control device produces an *actual control force* $u(t)$. For an ideal active element, $u(t) \equiv e(t)$. Across the element is a velocity differential $f(t)$, called the *shunt velocity*, which is $f(t) = f_1(t) - f_2(t)$.

The behavior of a semiactive force generator is determined by the relation between power flows associated with actual and ideal controls $u(t)$ and $e(t)$. The *actual control power* flowing into the element is

$$P(t) = u(t)f(t) \tag{1}$$

and $P(t)$ is positive when power is absorbed by the force generator. A *characteristic power* $\hat{P}(t)$ is the control power associated with the ideal active control $e(t)$:

$$\hat{P}(t) = e(t)f(t) \tag{2}$$

For an active element, $P(t) \equiv \hat{P}(t)$. Whenever $f(t)$ is nonzero, the force generator impedances are

$$R(t) = u(t)/f(t)$$

and

$$\hat{R}(t) = e(t)/f(t) \tag{3}$$

Both $R(t)$ and $\hat{R}(t)$ are time-varying resistances, and from Eqs. (1-3) the power flows are

$$P(t) = R(t)f^2(t)$$
$$\hat{P}(t) = \hat{R}(t)f^2(t) \tag{4}$$

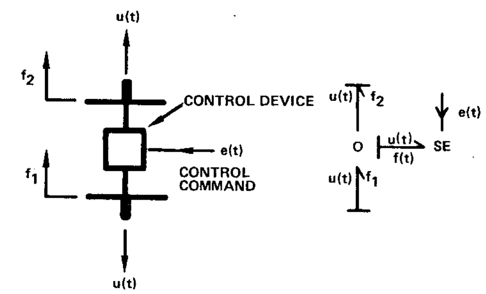

Fig. 1 Force-generating element and bond graph.

and the signs of $P(t)$ and $\hat{P}(t)$ are determined by $R(t)$ and $\hat{R}(t)$, respectively. In an ideal active force generator, $R(t) \equiv \hat{R}(t)$. However, in a semiactive element, thermodynamic irreversibility requires that $R(t)$ is positive semidefinite, and from Eq. (4) an inequality constraint on control power must exist

$$P(t) = R(t)f^2(t) \geq 0 \text{ when } R(t) \geq 0 \tag{5}$$

This constraint defines a semiactive force generator and the relation between actual and characteristic control powers is

$$P(t) = \begin{cases} \hat{P}(t), \hat{P}(t) > 0 \\ 0, \hat{P}(t) \leq 0 \end{cases} \tag{6}$$

Dividing the above expressions by nonzero $f(t)$ gives the constrained semiactive control

$$u(t)|_{f(t)\neq 0} = S[\hat{P}(t)]e(t) \tag{7}$$

where $S[\alpha]$ is the unit step function defined by

$$S[\alpha] = \begin{cases} 1, \alpha > 0 \\ 0, \alpha \leq 0 \end{cases} \tag{8}$$

This control is piecewise-constant and *bimodal.*

The state equation for a linear, stationary dynamic system with additive semiactive control is derived using Eq. (7) and the general state-space form

$$\dot{x}(t) = Ax(t) + Bu(t) + Gw(t) \tag{9}$$

where $x(t)$ is an N vector of linearly independent dynamic variables, $u(t)$ is an M vector of control inputs, and $w(t)$ is an R vector of disturbance inputs. The case where $u(t)$ is a linear state variable feedback (LSVF) semiactive control is now developed. Define an M vector of LSVF controls $e(t)$ such that

$$e(t) = K(t)x(t) \tag{10}$$

where $K(t)$ is an $M \times N$ matrix of control gains that may be time varying. For the ith controller, let

$$e_i(t) = K_i^T(t)x(t) \quad i = 1, \ldots, M \tag{11}$$

and $K_i^T(t)$ is the ith row of $K(t)$.† From Eqs. (1) and (2), the actual and characteristic powers associated with each element are

$$P_i(t) = u_i(t)f_i(t)$$

$$\hat{P}_i(t) = e_i(t)f_i(t) \quad i = 1, \ldots, M \tag{12}$$

where $f_i(t)$ is found by observing state and disturbance variables

$$f_i(t) = C_i^T x(t) + D_i^T w(t), \quad i = 1, \ldots, M \tag{13}$$

C_i^T and D_i^T are constant N and R vectors, respectively. From Eqs. (11-13), the characteristic powers are

$$\hat{P}_i(t) = x^T(t)K_i(t)[C_i^T x(t) + D_i^T w(t)] \quad i = 1, \ldots, M \tag{14}$$

From Eqs. (7) and (11), each semiactive element produces control inputs

$$u_i(t)|_{f_i(t)\neq 0} = S[\hat{P}_i(t)]e_i(t) = S[\hat{P}_i(t)]K_i^T(t)x(t)$$

$$i = 1, \ldots, M \tag{15}$$

†[ ]^T denotes either a row vector or matrix transposition.

Using this definition in Eq. (9), the state equation with M bimodal semiactive controls becomes

$$\dot{x}(t) = \left\{A + \sum_{i=1}^{M} B_i K_i^T(t) S[\hat{P}_i(t)]\right\} x(t) + Gw(t) \tag{16}$$

where B_i is the ith column of B. The term in braces in Eq. (16) is a *bilinear form*[13] of the system's dynamics matrix representing the *piecewise-linear* dynamics introduced by the semiactive controls. It is seen that the system closed-loop eigenvalues and eigenvectors change discontinuously whenever a $\hat{P}_i$ changes sign. Although $\dot{x}(t)$ is discontinuous at the switching points, $x(t)$ is continuous as long as $w(t)$ and the system eigenvalues remain bounded.

Equations (15) and (16) do not apply whenever any of the M shunt velocities $f_i(t)$ are zero at some time t. In particular, if $f_j(t) = 0$ *and* $\dot{f}_j(t) = 0$, then $u_j(t)$ is the force producing the *holonomic constraint*[14]

$$f_j(t) = C_j^T x(t) + D_j^T w(t) = 0 \tag{17}$$

If this constraint acts over the interval $t_0 \leq \tau < t_1$ then

$$f_j(\tau) = 0 \text{ and } \dot{f}_j(\tau) = 0 \tag{18}$$

Differentiating Eq. (13) gives

$$\dot{f}_j(\tau) = C_j^T \dot{x}(\tau) + D_j^T \dot{w}(\tau) \tag{19}$$

Whenever Eqs. (17) and (18) apply for the jth semiactive element, then $u_j(\tau) = \bar{u}_j(\tau)$ with $\bar{u}_j(\tau)$ denoting the holonomic constraint force at time $t = \tau$. When a single semiactive element generates a holonomic constraint, an expression for $\bar{u}_j(\tau)$ is found by writing the dynamics matrix in Eq. (16) exclusive of the contribution of $u_j(\tau)$

$$A_j(\tau) = A + \sum_{\substack{i=1 \\ i \neq j}}^{M} B_i \{K_i^T(\tau) S[\hat{P}_i(\tau)]\} \tag{20}$$

Using $A_j(\tau)$ in Eq. (9), the state equation becomes

$$\dot{x}(\tau) = A_j(\tau)x(\tau) + B_j \bar{u}_j(\tau) + Gw(\tau) \tag{21}$$

and from Eqs. (18), (19), and (21) write

$$C_j^T\{A_j(\tau)x(\tau) + B_j \bar{u}_j(\tau) + Gw(\tau)\} + D_j^T \dot{w}(\tau) = 0 \tag{22}$$

The holonomic constraint force is

$$\bar{u}_j(\tau) = \lambda_j \{C_j^T A_j(\tau)x(\tau) + C_j^T G w(\tau) + D_j^T \dot{w}(\tau)\} \tag{23a}$$

where

$$\lambda_j = -(C_j^T B_j)^{-1} \tag{23b}$$

It can be shown that λ_j is a positive constant when f_j is determined by the system inertial velocities. If there are two or more semiactive elements simultaneously providing holonomic constraints, the above procedure generalizes to yield a simultaneous solution for the set of $\bar{u}_j(\tau)$.

For the special case of a single holonomic constraint, the system state equation from Eqs. (21) and (23) is

$$\dot{x}(\tau) = \{I + \lambda_j B_j C_j^T\}\{A_j(\tau)x(\tau) + Gw(\tau)\} + \lambda_j B_j D_j^T \dot{w}(\tau) \tag{24}$$

where I is the $N \times N$ identity matrix. The dynamics matrix $\{I + \lambda_j B_j C_j^T\} A_j(\tau)$ must have rank $N-1$ because the holonomic constraint reduces from N to $N-1$ the number of linearly independent state variables.

Assuming $f_j(t_0)=0$ and $f_j(t_l)\neq 0$, the behavior of $u_j(t)$ is now described for $t_0\leq\tau\leq t_l$. In this analysis, the existence of a functional form of $\dot{f}_j(\tau)$ and the continuity of $\tilde{u}_j(\tau)$ are assumed which require at least the piecewise-continuity of $\dot{x}(t)$ and $\dot{w}(t)$ for $t=\tau$. For $\dot{x}(\tau)$ to be continuous, the remaining controls $u_i(t)$, $i=1,\ldots, M$ with $i\neq j$, must be continuous interior to the interval. An expression permitting $u_j(\tau)$ to assume any of its possible values‡ is

$$u_j(\tau)\,|_{f_j(\tau)=0}=S_1(\tau)\tilde{u}_j+S_2(\tau)\{e_j(\tau)-\tilde{u}_j(\tau)\} \tag{25}$$

where

$$S_1(\tau)=S[\xi_j(\tau)] \quad S_2(\tau)=S[\zeta_j(\tau)] \tag{26}$$

and $S[\cdot]$ is defined in Eq. (8). The control $u_j(\tau)$ is piecewise-constant and *trimodal*. The functions $\xi_j(\tau)$ and $\zeta_j(\tau)$ are switching functions determined from the following arguments. In Eq. (25), find that

$$u_j(\tau)=\tilde{u}_j(\tau)\begin{cases} S_1(\tau)=1\\ S_2(\tau)=0\end{cases} \tag{27a}$$

$$u_j(\tau)=e_j(\tau)\begin{cases} S_1(\tau)=1\\ S_2(\tau)=1\end{cases} \tag{27b}$$

and

$$u_j(\tau)=0\qquad\begin{cases} S_1(\tau)=0\\ S_2(\tau)=0\end{cases} \tag{27c}$$

When $f_j(\tau)=0$, $P_j(\tau)=0$, but the behavior of $u_j(t)$ at $t=\tau+\epsilon$, $\epsilon>0$, may be predicted from $\dot{P}_j(\tau)$, where

$$\dot{P}_j(\tau)\,|_{f_j(\tau)=0}=u_j(\tau)\dot{f}_j(\tau) \tag{28}$$

An expression for $\dot{f}_j(\tau)$ is obtained by formally replacing $\tilde{u}_j(\tau)$ in Eq. (21) with $u_j(\tau)$ from Eq. (25). Substituting the result into Eq. (19) and using Eq. (23) gives

$$\dot{f}_j(\tau)=\frac{1}{\lambda_j}\{\tilde{u}_j(\tau)(1-S_1(\tau))-(e_j(\tau)-\tilde{u}_j(\tau))S_2(\tau)\} \tag{29}$$

Using Eqs. (25), (28), and (29), a form for $\dot{P}_j(\tau)$ containing S_1 and S_2 is

$$\dot{P}_j=\frac{1}{\lambda_j}(e_j-\tilde{u}_j)\{\tilde{u}_j-2\tilde{u}_jS_1-(e_j-\tilde{u}_j)S_2\}S_2 \tag{30}$$

Evidently, $\dot{P}_j(\tau)=0$ whenever $S_2=0$ ($\zeta_j(\tau)\leq 0$).

The switching functions are found by considering the behavior of $\dot{P}_j(\tau)$ when $u_j(\tau)=e_j(\tau)$. Note that the other cases from Eq. (27) are also allowed by permitting $e_j(\tau)=\tilde{u}_j(\tau)$ or $e_j(\tau)=0$. With $S_1=S_2=1$, Eq. (30) becomes

$$\dot{P}_j(\tau)=\frac{1}{\lambda_j}\{e_j(\tau)\tilde{u}_j(\tau)-e_j^2(\tau)\} \tag{31}$$

Since Eq. (5) requires $P_j(\tau)$ to be positive semidefinite, it follows that $\dot{P}_j(\tau)\geq 0$ when $P_j(\tau)=0$. When $\dot{P}_j(\tau)>0$, Eq. (31) requires

$$e_j(\tau)\tilde{u}_j(\tau)-e_j^2(\tau)>0 \tag{32}$$

which is true only if

$$e_j(\tau)\tilde{u}_j(\tau)>0 \tag{33a}$$

‡That is, $\tilde{u}_j(\tau)$, $e_j(\tau)$, or zero.

and

$$|\tilde{u}_j(\tau)|>|e_j(\tau)| \tag{33b}$$

In this case, $u_j(\tau)=e_j(\tau)$, and $e_j(\tau)$ is neither zero nor $\tilde{u}_j(\tau)$ from Eqs. (32) and (33). When $\dot{P}_j(\tau)=0$,

$$e_j(\tau)\tilde{u}_j(\tau)-e_j^2(\tau)=0 \tag{34}$$

and this is true if either $u_j(\tau)=e_j(\tau)=\tilde{u}_j(\tau)$, in which case Eq. (33a) is satisfied, or $u_j(\tau)=e_j(\tau)=0$ which requires

$$e_j(\tau)\tilde{u}_j(\tau)=0 \tag{35}$$

Regardless of the value of $e_j(\tau)\tilde{u}_j(\tau)$, which discriminates $e_j(\tau)=0$ from the other cases, $\dot{P}_j(\tau)=0$ whenever Eq. (34) obtains. From the above results, the functions $(e_j\tilde{u}_j-e_j^2)$ and $(e_j\tilde{u}_j)$ are found to discriminate between the three possibilities for $u_j(\tau)$. If for S_1

$$\xi_j(\tau)=e_j(\tau)\tilde{u}_j(\tau)\,|_{f_j(\tau)=0} \tag{36a}$$

and for S_2

$$\zeta_j(\tau)=(e_j(\tau)\tilde{u}_j(\tau)-e_j^2(\tau)\,|_{f_j(\tau)=0} \tag{36b}$$

the choice of $u_j(\tau)$ by Eq. (25) is consistent with the above conclusions. The definitions of $\xi_j(\tau)$ and $\zeta_j(\tau)$ in Eq. (36) are also consistent for cases where $S_1\neq S_2$ and preclude the possibility that $\dot{P}_j(\tau)<0$ when $P_j(\tau)=0$. Specifically, Eq. (27) gives $u_j(\tau)$ as the holonomic constraint force $\tilde{u}_j(\tau)$ whenever

$$\xi_j(\tau)>0 \text{ and } \zeta_j\leq 0 \tag{37a}$$

and $u_j(\tau)=0$ whenever

$$\xi_j(\tau)<0 \text{ and } \zeta_j(\tau)<0 \tag{37b}$$

When $t=t_l$, conditions in Eq. (37a) are violated and the holonomic constraint is relaxed.

The general form of the state equation for the piecewise-linear dynamics of a system with LSVF semiactive control is now expressed. Calculating all $u_i(t)$ for which $f_i(t)$ is nonzero by Eq. (15) and all $u_i(t)$ for which $f_i(t)$ is zero using Eqs. (25), (26), and (36), Eq. (9) has the bilinear form

$$\begin{aligned}\dot{x}(t)=&\left[A+\sum_{i=1}^{M}B_iK_i^T(t)S[\hat{P}_i(t)]\right]x(t)\\ &+\sum_{i=1}^{M}B_i(1-S[f_i^2(t)])u_i(t)\,|_{f_i(t)=0}+G\,w(t)\end{aligned} \tag{38}$$

A system described by Eq. (38) is piecewise-linear with linear-dependencies in the state vector produced by periodic application of holonomic constraints. Because the state-dependent holonomic constraint forces make the Nth order equation appear to have infinitely stiff elements, direct numerical solution of Eq. (38) is impractical and exhibits numerical instabilities. If n holonomic constraints apply at time t, one method of solution of Eq. (38) is to transform the state equation in $x(t)$ into a constrained N-n subspace $\hat{x}(t)$.[15] The elements of $\hat{x}(t)$ will be linearly independent and constraints are incorporated algebraically into the equation of state rather than numerically as in a direct solution of Eq. (38).

Simplified Dynamics

In two circumstances, the dynamics of a system with LSVF semiactive control may be expressed in forms less complex than Eq. (38). In one case, the active and semiactive controls are indistinguishable, and system dynamics are represented by

Eq. (9). In the other case, the holonomic constraint mode may be ignored and the semiactive control is bimodal as in Eq. (16).

From Eq. (15), the semiactive control $u_i(t)$ is identical to the active control $e_i(t)$ when $\hat{P}_i(t)$ is positive-semidefinite for all t. Although this definition is valid only when the zero of $\hat{P}_i(t)$ is produced by $e_i(t)$, its validity may be extended if every zero of $f_i(t)$ is also a zero of $e_i(t)$. The positive semi-definiteness of $\hat{P}_i(t)$ and this latter condition together require that

$$e_i(t) = \hat{R}_i(t) f_i(t) \tag{39}$$

where $\hat{R}_i(t)$ is real and positive semidefinite. If at time t for any nonzero $\hat{R}_i(t)$ $e_i(t) = 0$ when $f_i(t) = 0$, then from Eqs. (11) and (17)

$$\boldsymbol{K}_i^T(t)\boldsymbol{x}(t) = \boldsymbol{C}_i^T\boldsymbol{x}(t) + \boldsymbol{D}_i^T\boldsymbol{w}(t) = 0 \tag{40}$$

Since $\boldsymbol{w}(t)$ is independent of $\boldsymbol{x}(t)$, Eq. (40) is true in general if and only if

$$\boldsymbol{D}_i^T\boldsymbol{w}(t) \equiv 0 \tag{41}$$

This condition is satisfied when the ith semiactive force generator is either located remote from external disturbances or attached to a stationary frame. In either case, the shunt velocity is a function only of state: $f_i(t) = \boldsymbol{C}_i^T\boldsymbol{x}(t)$. Making use of the linear independence of state variables $\boldsymbol{x}(t)$ in Eq. (9) and using Eq. (39-41), the required LSVF control is

$$\boldsymbol{K}_i^T(t) = \hat{R}_i(t)\boldsymbol{C}_i^T \tag{42}$$

The active and semiactive feedback control gains are proportional to the shunt velocity state observer by the resistive coefficient $\hat{R}_i(t)$. When the control is given by Eq. (42) and $\hat{R}_i(t)$ is positive semidefinite, Eq. (9) with $\boldsymbol{u}(t) \equiv \boldsymbol{e}(t)$ describes system dynamics for both active and semiactive LSVF control.

When $\hat{R}_i(t)$ has arbitrary sign, control according to Eq. (39) is an Identically-Located Sensor and Manipulator (or ILSM) control.[16] A semiactive ILSM control scheme has been studied[11] using a similar example system as will be discussed in this paper. When $f_i(t)$ is a system velocity referenced to a stationary frame, Eq. (42) is a special case of ILSM control given the descriptive name *Skyhook Damping*.[9] In this case, if $\hat{R}_i(t)$ is a positive constant, Eq. (42) represents the control produced by attaching a simple viscous damper between a point in a vibrating system and an inertial frame.

Under conditions where the impulse due to holonomic constraint forces is negligible, a bimodal representation of the semiactive control provides simplification of the system state equations. Equation (16) is a bimodal form which has analytic and numerical advantages over Eq. (38). Of primary advantage, the semiactive controls $\boldsymbol{u}(t)$ are defined by the simple switching function in Eq. (15) and the elements of the state vector remain linearly independent.

The impulse due to holonomic constraint forces may be made arbitrarily small if conditions are found where every semiactive control $u_i(t)$ remains bounded as every interval over which $u_i(t) = \bar{u}_i(t)$ is made arbitrarily small. Denote this interval as $\epsilon = t_I - t_0$, when the holonomic constraint is applied at $t = t_0$. Equations (36) and (37a) specify

$$\xi_j(t_0) = e_j(t_0)\bar{u}_j(t_0) > 0 \tag{43a}$$

and

$$\zeta_j(t_0) = e_j(t_0)(\bar{u}_j(t_0) - e_j(t_0)) \le 0 \tag{43b}$$

The constraint is relaxed at $t = t_I$ when either

$$\xi_j(t_I) = e_j(t_I)\bar{u}_j(t_I) \le 0 \tag{44a}$$

or

$$\zeta_j(t_I) = e_j(t_I)(\bar{u}_j(t_I) - e_j(t_I)) > 0 \tag{44b}$$

As ϵ approaches zero, if $e_j(\tau)$ is continuous, then sufficient conditions to relax the constraint are either a sign change on $\bar{u}_j(t)$ during the interval ϵ or finding $\zeta_j(t_I) > 0$ when $\xi_j(t_I) > 0$. The former condition is satisfied in general if the spectrum of $\bar{u}_j(t)$ is dominated by densities near $\omega_0 = \pi/\epsilon$. The latter condition is equivalent to $(\bar{u}_j(t_I))^2 > (e_j(t_I))^2$ when $\bar{u}_j(t_I)$ and $e_j(t_I)$ have the same sign. In the following discussion, it is found that either or both of the above conditions apply when the disturbance vector $\boldsymbol{w}(t)$ contains broad-band noise elements.

From Eq. (23a), $u_j(t)$ is seen to contain the term $\boldsymbol{D}_j^T\dot{\boldsymbol{w}}(t)$. Let the disturbance-dependent term in the shunt velocity, $\boldsymbol{D}_j^T\boldsymbol{w}(t)$, be Gaussian band-limited white noise with mean square spectral density S_0 below a cutoff frequency ω_c. The spectra of $\boldsymbol{D}_j^T\boldsymbol{w}(t)$ and $\boldsymbol{D}_j^T\dot{\boldsymbol{w}}(t)$ are, respectively,

$$S_{D_j^T w(t)}(\omega) = \begin{cases} S_0, |\omega| \le \omega_c \\ 0, |\omega| > \omega_c \end{cases} \tag{45a}$$

and

$$S_{D_j^T \dot{w}(t)}(\omega) = \begin{cases} \omega^2 S_0, |\omega| \le \omega_c \\ 0, |\omega| > \omega_c \end{cases} \tag{45b}$$

Denoting an expected value by $E[\cdot]$, the mean-square value of $\boldsymbol{D}_j^T\dot{\boldsymbol{w}}(t)$ is

$$E[(\boldsymbol{D}_j^T\dot{\boldsymbol{w}}(t))^2] = \int_{-\omega_c}^{\omega_c} \omega^2 S_0 \mathrm{d}\omega = \frac{2\omega_c^3}{3} S_0 \tag{46}$$

and can be made arbitrarily large by increasing the cutoff frequency. If the system with semiactive control is stable with bounded controls $\boldsymbol{e}(t)$, then the norm of $\boldsymbol{x}$ is bounded and $E[(\bar{u}_j(t))^2]$ will be dominated by $E[(\boldsymbol{D}_j^T\dot{\boldsymbol{w}}(t))^2]$ for large ω_c. The interpretation of $\bar{u}_j(t) \sim \lambda_j \boldsymbol{D}_j^T\dot{\boldsymbol{w}}(t)$ is that $\bar{u}_j(t)$ is the force required to impart an inertial acceleration $\boldsymbol{D}_j^T\dot{\boldsymbol{w}}(t)$. It can be shown that λ_j has units of inertia when system inertial elements provide the independent velocity variables observed by $\boldsymbol{C}_j^T$ in Eq. (13).

Taking ω_c sufficiently large for each $\boldsymbol{D}_j^T\boldsymbol{w}(t)$, $j = 1, \ldots, M$, then

$$E[(\bar{u}_j(t))^2] \gg E[(e_j(t))^2] \quad j = 1, \ldots, M \tag{47}$$

and the probability that $(\bar{u}_j(t))^2 < (e_j(t))^2$ is very small. This is equivalent to the probability that $\zeta_j(t) \le 0{:}p]\zeta_j(t) \le 0]$. The probability that at time t the jth semiactive controller is enforcing a holonomic constraint is

$$p[u_j(t) = \bar{u}_j(t)] = p[\zeta_j(t) \le 0] \cdot p[\xi_j(t) > 0] \tag{48}$$

which can be made arbitrarily small through the choice of ω_c. Predominantly bimodal behavior of systems with semiactive control occurs whenever band-limited white noise may be used to characterize system inputs. The velocity spectrum of inputs to ground vehicle suspension systems may be modeled in this manner.[3,17]

Example System: Dynamics of a Flexible Ground Vehicle

A simple model of the planar rigid and elastic body dynamics of a flexible vehicle is shown along with its bond graph[12] in Fig. 2. Using this system, a performance comparison will be made between passive, active, and semiactive controls. The vehicle is modeled as a uniform elastic continuum supported near each end by a suspension unit con-

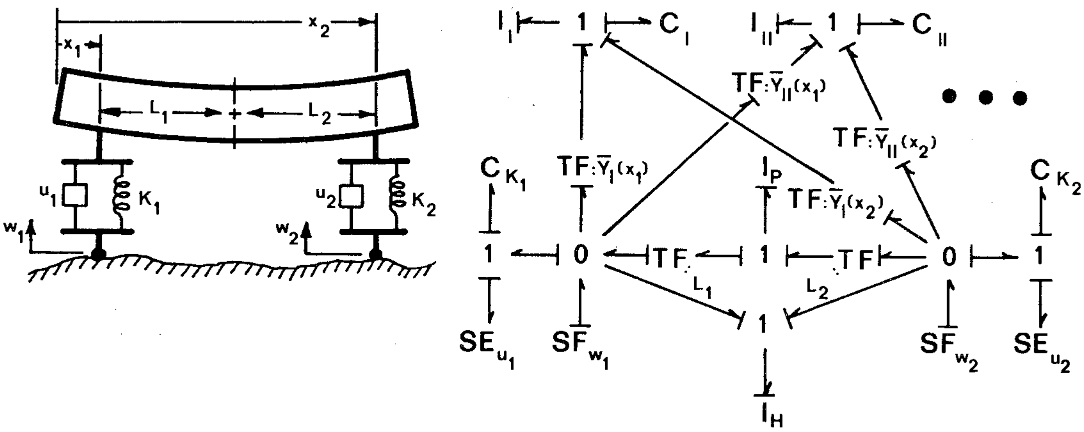

Fig. 2 Schematic of simple flexibld vehicle and bond graph.

taining a linear spring and a force generator. The latter is taken alternatively to be a linear viscous damper, an active and semiactive element. The model includes heave and pitch motions and the two lowest beam-bending modes. Motion of the translating vehicle is excited by guideway roughness appearing as velocity input to the suspensions.

The suspensions produce concentrated loads at beam stations $x=x_1$ and $x=x_2$ which excite undamped rigid and elastic body modes. The displacement of a point on the beam $y(x,t)$ is represented by a combination of rigid and elastic body displacements

$$y(x,t)=q_H+(x-L/2)q_p+\bar{Y}_I(x)q_I(t)+\bar{Y}_{II}(x)q_{II}(t) \quad (49)$$

where q_H is the heave displacement, q_p the pitch angle, and $\bar{Y}_i$ the shape function for the ith bending mode. The mass center is at $x=L/2$. The shape functions for rigid and elastic body modes are shown in the positive sense in Fig. 3. The heave and first bending modes are symmetric about the mass center while pitch and the second bending mode are antisymmetric. The variable $q_i(t)$ is the time function for undamped, forced oscillation in the ith mode

$$q_i(t)=\frac{1}{\omega_{Ni}^2}\left[\int_0^L F(x,t)\,\bar{Y}_i(x)\mathrm{d}x-\ddot{q}_i(t)\right] i=\mathrm{I},\ \mathrm{II} \quad (50)$$

$F(x,t)$ represents suspension forces, and ω_{N_i} is an undamped natural frequency. In Eq. (50), $\bar{Y}_i(x)$ acts as an admittance function, and suspension forces at x_1 and x_2 excite bending through the transformer (TF) elements with moduli $\bar{Y}_i(x)$ in the bond graph in Fig. 2. Here, the I_i and C_i elements characterize the inertia and stiffness of each mode, m_i and κ_i, respectively. For the rigid body dynamics, I_H represents the heave inertia M_H, and I_P the centroidal pitch moment of inertia J. L_1 and L_2 are the suspension displacements from the mass center and TF elements produce the pitch moment of the suspension forces. The model is linearized by restricting pitch to small angles.

Guideway unevenness can be characterized by a velocity normal to the surface and related to vehicle speed and surface condition. For a variety of surfaces including runways, road- and railbeds, the velocity power spectrum may be approximated by white noise.[3,17] Primary suspension systems such as pneumatic tires and air cushions are low-pass filters which provide band-limiting of the guideway velocity spectrum.[17] When the cutoff frequency is sufficiently high, the semiactive control will be bimodal. In this model, the effect of primary suspensions is included by the band-limited white noise velocities $w_1(t)$ and $w_2(t)$, which appear directly across the semiactive elements. When the vehicle translates at constant velocity V to the left in Fig. 2, $w_1(t)$ and $w_2(t)$ are delay correlated:

$$w_2(t+(L_1+L_2)/V)=w_1(t) \quad (51)$$

From the bond graph, the system state equation in the form of Eq. (9) is written[12]

$$\begin{vmatrix}\dot{q}_1\\ \dot{q}_2\\ \dot{p}_H\\ \dot{p}_P\\ \dot{q}_I\\ \dot{p}_I\\ \dot{q}_{II}\\ \dot{p}_{II}\end{vmatrix}=\begin{vmatrix}0 & 0 & \frac{-1}{M_H} & \frac{L_1}{J} & 0 & \frac{\bar{Y}_I(x_1)}{m_I} & 0 & \frac{-\bar{Y}_{II}(x_1)}{m_{II}}\\ 0 & 0 & \frac{-1}{M_H} & \frac{-L_2}{J} & 0 & \frac{-\bar{Y}_I(x_2)}{m_I} & 0 & \frac{-\bar{Y}_{II}(x_2)}{m_{II}}\\ K_1 & K_2 & 0 & 0 & 0 & 0 & 0 & 0\\ -K_1L_1 & K_2L_2 & 0 & 0 & 0 & 0 & 0 & 0\\ 0 & 0 & 0 & 0 & 0 & \frac{1}{m_I} & 0 & 0\\ K_1\bar{Y}_I(x_1) & K_2\bar{Y}_I(x_2) & 0 & 0 & -\kappa_I & 0 & 0 & 0\\ 0 & 0 & 0 & 0 & 0 & 0 & 0 & \frac{1}{m_{II}}\\ K_1\bar{Y}_{II}(x_1) & K_2\bar{Y}_{II}(x_2) & 0 & 0 & 0 & 0 & -\kappa_{II} & 0\end{vmatrix}\begin{vmatrix}q_1\\ q_2\\ p_H\\ p_P\\ q_I\\ p_I\\ q_{II}\\ p_{II}\end{vmatrix}+\begin{vmatrix}0 & 0\\ 0 & 0\\ 1 & 1\\ -L_1 & L_2\\ 0 & 0\\ \bar{Y}_I(x_1) & \bar{Y}_I(x_2)\\ 0 & 0\\ \bar{Y}_{II}(x_1) & \bar{Y}_{II}(x_2)\end{vmatrix}\begin{vmatrix}u_1\\ u_2\end{vmatrix}+\begin{vmatrix}1 & 0\\ 0 & 1\\ 0 & 0\\ 0 & 0\\ 0 & 0\\ 0 & 0\\ 0 & 0\\ 0 & 0\end{vmatrix}\begin{vmatrix}w_1\\ w_2\end{vmatrix} \quad (52)$$

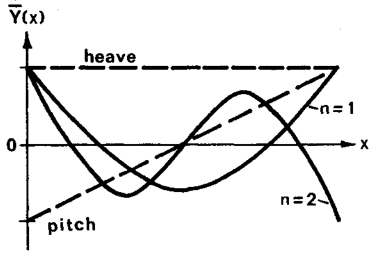

Fig. 3 Rigid and elastic body mode shapes.

Variables p and q represent system momenta and displacements, respectively, q_1 and q_2 are suspension deflections and in Eq. (49)

$$q_H = -(q_1 + q_2)/2$$

$$q_p = (q_1 - q_2)/(L_1 + L_2) \tag{53}$$

The control objective is a decoupled control between symmetric and antisymmetric modes which adds damping to each mode. The open-loop system is decoupled by specifying $K_1 = K_2$ and $L_1 = L_2$. In Eq. (52), $\boldsymbol{u}(t)$ is the actual control produced in turn by active, semiactive, and passive control. The active and semiactive controls are defined in Eqs. (11) and (15), respectively. Identical $\boldsymbol{K}$ matrices with constant coefficients are used for both active and semiactive controls. For the passive control example, linear viscous dampers with damping coefficients b are placed in the suspensions. The passive control forces are

$$u_i(t) = bf_i(t) \quad i = 1,2 \tag{54}$$

where $f_1(t) = \dot{q}_1(t)$ and $f_2(t) = \dot{q}_2(t)$ in Eq. (52). In the example passive system, the choice of b represents a selection of heave and bending mode time constants comparable to the slowest time constant in the (overdamped) pitch mode. The control objectives using active, semiactive, and passive controls are summarized in Table 1. The resulting semiactive controls when one or both characteristic powers are negative are also presented. Due to the symmetry of the system and controls, closed-loop eigenvalues are the same independent of the semiactive element for which $S[\hat{P}_i]$ is zero. The system eigenvectors are nonidentical.

Numerical Results and Discussion

The performance of the system in Fig. 2 with the controls in Table 1 was evaluated by digital simulation. The system state equation (52) was solved directly for active and passive controls and in the form of Eq. (16) for the semiactive control. Inputs $w_1(t)$ and $w_2(t)$ had identical time histories for each example. The inputs were Gaussian white noise with unity rms spectral densities passed through a second-order lag having a corner frequency at 50 Hz. This was the Nyquist frequency for the sampled response data, and attenuation of the input spectra above 50 Hz inhibited *aliasing* in the spectral analyses.[18] In Eq. (51), the delay-correlation between $w_1(t)$ and $w_2(t)$ was 0.722 sec. This is representative of a vehicle with a 10 m wheelbase $(L_1 + L_2)$ travelling at 50 km/hr (V).

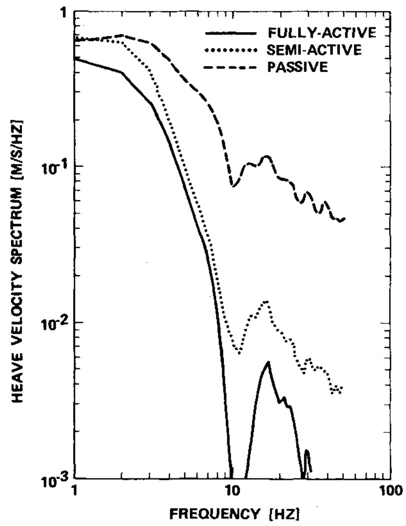

Fig. 4 Heave rms velocity spectra.

The rms spectra for velocity responses in the rigid and elastic body modes and for control forces $u_1(t)$ appear in Figs. 4-8§. The spectra were produced from a single sample containing 2000 observations using techniques described in Ref. 18. Clearly visible in the responses are the coupling between modes of like symmetry. The coupling of heave with the first bending mode (10 Hz) and pitch with the second bending mode (27.7 Hz) are pronounced in Figs. 4 and 5, respectively. Below 6 Hz in all modes, the response spectra for semiactive control resemble the active control spectra. However, above 6 Hz a degradation is seen in the effectiveness of the semiactive control compared with active control. The response spectra at high frequency for semiactive control appear similar to the passive control responses but the latter are larger by an order-of-magnitude. Table 2 presents the rms responses in each mode and two performance indices. Q_1 represents the root of the sum of mean square velocity responses in each mode normalized by the result for active control

$$Q_1 = \frac{1}{0.864}\,[\bar{v}_H^2 + \bar{v}_P^2 + \bar{v}_I^2 + \bar{v}_{II}^2]^{0.5} \tag{55}$$

§A linear velocity for pitch is taken as the pitch component of $\dot{q}_1$ in Eq. (52).

Table 1 Control objectives for example systems

			Heave		Pitch		Bending I		Bending II	
Configuration	$S[\hat{P}_1]$	$S[\hat{P}_2]$	ζ^a	$f_N{}^b$	ζ	f_N	ζ	f_N	ζ	f_N
Open-loop system	–	–	0.0	1.96	0.0	3.98	0.0	10.2	0.0	27.7
LSVF active control	–	–	0.707	1.96	0.50	3.98	0.60	10.2	0.60	27.7
LSVF semiactive control	0	0	0.0	1.96	0.0	3.98	0.0	10.2	0.0	27.7
	1	1	0.707	1.96	0.50	3.98	0.60	10.2	0.60	27.7
	1	0	0.39	2.18	0.24	3.64	0.32	10.9	0.31	25.4
	0	1								
Passive control	–	–	0.74	2.05	1.55	4.15	0.15	9.72	0.05	27.0

[a]Damping ratio. [b]Undamped natural frequency, Hz.

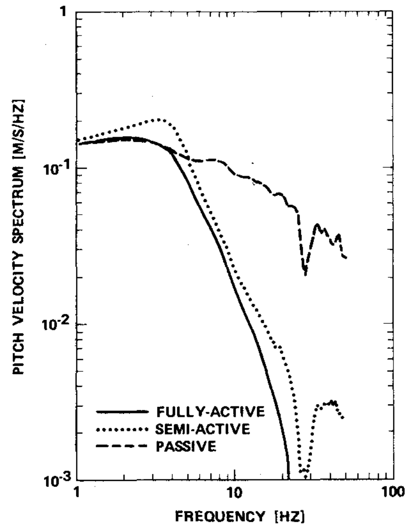

Fig. 5 Pitch rms velocity spectra.

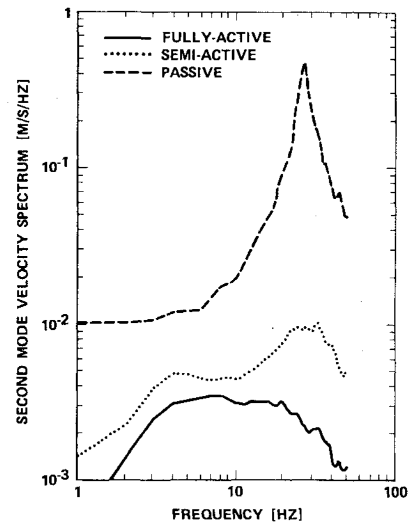

Fig. 7 Second bending mode rms velocity spectra.

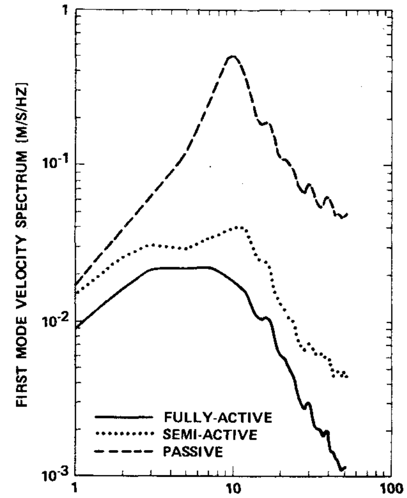

Fig. 6 First bending mode rms velocity spectra.

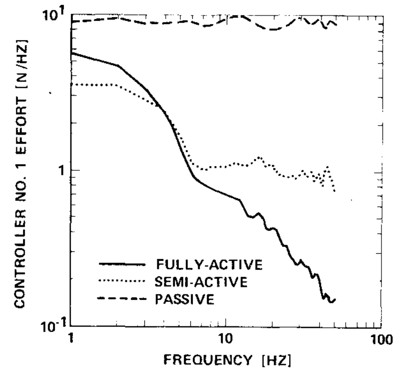

Fig. 8 Control rms force spectra.

This index is most sensitive to heave and pitch performance due to larger numerical values of $\bar{v}_H$ and $\bar{v}_p$. Q_2 provides a measure based on the relative performance in each mode compared to the active control result

$$Q_2 = \frac{1}{2}\left[\left(\frac{\bar{v}_H}{0.797}\right)^2 + \left(\frac{\bar{v}_P}{0.326}\right)^2 + \left(\frac{\bar{v}_I}{0.074}\right)^2 + \left(\frac{\bar{v}_{II}}{0.017}\right)^2\right]^{1/2} \tag{56}$$

Based on Figs. 4-7 and Table 2, the semiactive control is found to be nearly as effective as the active control and is clearly superior to the passive control in all system modes of vibration.

Table 3 provides a statistical measure of the influence of the power flow constraint Eq. (6) on the behavior of the semiactive control. Although both semiactive elements simultaneously generated the LSVF control during only 33% of the simulation interval, one or both elements were active during 82% of the interval. The characteristic power for each controller has components at high frequency due to the white noise in the shunt velocity. This results in rapid switching of the semiactive control between the LSVF control force and zero producing a "chopped" LSVF control with reduced effectiveness at high frequencies. This accounts for the increased vibrational amplitudes in all modes producing larger LSVF control signals than are found in the fully active system. Above 6 Hz, the spectrum of the semiactive control $u_I(t)$ in Fig. 8 resembles the spectrum of the noise input $w_I(t)$ rather than the active LSVF control spectrum. Because the shunt velocities for the passive dampers are dominated by $w_I(t)$, the spectrum of passive control force $u_I(t)$ appears as nearly white noise with an rms spectral density of b, the passive damping coefficient. This explains the observed correlation of passive and semiactive velocity response spectra above 6 Hz.

Conclusions

Equations in state variable form are developed to describe dynamics of a general linear system containing semiactive force generators. The control force produced by a semiactive element depends on the control law, the velocity difference across the element, and a control power constraint. The semiactive control has three distinct modes that introduce piecewise-linear dynamics and intermittant constraints among the system state variables. Whenever the control permits dissipation of system energy, semiactive control is indistinguishable from control using active force generators. At other times, the control power constraint requires the

Table 2 Root mean square responses of example systems

Configuration	$\bar{v}_H{}^a$	$\bar{v}_P{}^a$	$\bar{v}_I{}^a$	$\bar{v}_{II}{}^a$	$Q_1{}^b$	$Q_2{}^c$
LSVF active control	0.797	0.326	0.074	0.017	1.00	1.00
LSVF semiactive control	1.11	0.417	0.136	0.050	1.38	1.98
Passive	1.50	0.515	1.23	1.08	2.64	32.8

[a] RMS velocities in heave, pitch, first, and second bending modes respectively (m/sec). [b] Performance index, see Eq. (55). [c] Performance index, see Eq. (56).

Table 3 Semiactive control statistics

Observed control states						Simulation
$S[\hat{P}]$	:	$u_1(t)$	$S[\hat{P}_2]$	:	$u_2(t)$	interval (%)
0		0	0		0	18
1		$e_1(t)$	0		0	25
0		0	1		$e_2(t)$	24
1		$e_1(t)$	1		$e_2(t)$	33

semiactive element to generate either no control force or the force required to maintain zero velocity across the element. Special cases are found in which the semiactive control is either always identical to active control or is bimodal with rapid switching between the desired control and zero control modes. Both cases are of practical importance and permit simplified descriptions of system dynamics.

The performance of passive, active, and semiactive vibration controls are compared in a system with multiple modes of vibration. Numerical analyses producing system response spectra show that at low frequencies active and semiactive controls produce comparable results. At high frequencies, the shape of the response spectra for passive and semiactive controls are similar, but the semiactive control produces better isolation by an order-of-magnitude. The overall performance of semiactive vibration control is judged comparable to active control and clearly superior to passive control. Based on these results, semiactive force generation merits consideration as an effective, self-powered vibration control. Analyses of practical applications of semiactive control are facilitated by the theory developed in this paper.

In conclusion, it should be noted that the constrained control produced when semiactive force generators implement an unconstrained optimal control is not necessarily optimal. For an optimal semiactive control, the control gain matrix $\boldsymbol{K}(t)$ must be derived using the *maximum principle* and the inequality constraint on semiactive control power.

References

[1] Corsetti, C. D. and Dillow, J. D., "A Study of the Practicality of Active Vibration Isolation Applied to Aircraft During the Taxi Condition," U.S. Air Force Flight Dynamics Laboratory, Tech. Report AFFDL-TR-71-159, July 1972.

[2] Hedrick, J. K., Billington, G. F., and Dreesbach, D. Q., "Analysis, Design, and Optimization of High Speed Vehicle Suspensions Using State Variable Techniques," *Transactions of the ASME, Journal of Dynamic Systems, Measurement, and Control*, Vol. 96, Series G, June 1974, pp. 193-203.

[3] Young, J. W. and Wormley, D. N., "Optimization of Linear Vehicle Suspensions Subjected to Simultaneous Guideway and External Force Disturbances," *Transactions of the ASME, Journal of Dynamic Systems, Measurement, and Control*, Vol. 95, Series G, June 1973, pp. 213-219.

[4] Paul, I. K. and Bender, E. K., "Partial Bibliography on Subjects Related to Active Vibration Isolation and Active Vehicle Suspensions," Engineering Projects Laboratory, M.I.T., 1966.

[5] Smith, R. E. and Lum, E.L.S., "Linear Optimal Theory Applied to Active Structural Bending Control," *Journal of Aircraft*, Vol. 5, Sept.-Oct. 1968, pp. 475-479.

[6] Karnopp, D. C. and Trikha, A. K., "Comparative Study of Optimization Techniques for Shock and Vibration Isolation," *Transactions of the ASME, Journal of Engineering for Industry*, Vol. 91, Series B, Nov. 1969, pp. 1128-1132.

[7] Sevin, E. and Pilkey, W. D., *Optimum Shock and Vibration Isolation*, Shock and Vibration Monograph #6, The Shock and Vibration Information Center, Naval Research Center, Washington, D. C., 1971.

[8] Crosby, M. J. and Karnopp, D., "The Active Damper – A New Concept for Shock and Vibration Control," *Shock and Vibration Bulletin*, Vol. 43, Part 4, June 1973, pp. 119-133.

[9] Karnopp, D., Crosby, M. J., Harwood, R. A., "Vibration Control Using Semiactive Force Generators," *Transactions of the ASME, Journal of Engineering for Industry*, Vol. 96, Series G, May 1974, pp. 619-626.

[10] Margolis, D. and Tylee, J. L., "Heave Mode Dynamics of a Tracked Air Cushion Vehicle Incorporating a Semi-Active Airbag Secondary Suspension," *Transactions of the ASME, Journal of Dynamic Systems, Measurement, and Control*, Vol. 97, Series G, Dec. 1975, pp. 399-407.

[11] Karnopp, D., Allen, R. R., "Semi-Active Control of Multi-Mode Vibratory Systems Using the ILSM Concept," *Transactions of the ASME, Journal of Engineering for Industry*, Vol. 98, Series B, Aug. 1976, pp. 914-918.

[12] Karnopp, D. C. and Rosenberg, R. C., *System Dynamics: A Unified Approach*, Wiley, New York, 1975.

[13] Mohler, R. R., *Bilinear Control Processes*, Academic Press, New York, 1973.

[14] Crandall, S. H., Karnopp, D. C., Kurtz, E. F., Jr., and Pridmore-Brown, D. C., *Dynamics of Mechanical and Electromechanical Systems*, McGraw-Hill, New York, 1968, p. 119.

[15] Allen, R. R., "The Dynamics of Multiple State-Space Systems," Ph.D. Dissertation, University of California, Davis, June 1975.

[16] Rockwell, T. H. and Lawther, J. M., "Theoretical and Experimental Results on Active Vibration Dampers," *Journal of Acoustical Society of America*, Vol. 36, Aug. 1964, pp. 1507-1515.

[17] Karnopp, D. C., "Applications of Random Process Theory to the Design and Testing of Ground Vehicles," *Transportation Research*, Vol. 2, Sept. 1968, pp. 269-278.

[18] Bendat, J. S., Piersol, A. G., *Measurement and Analysis of Random Data*, Wiley, New York, 1967.